THE ASTROPHYSICAL JOURNAL, 349:97–106, 1990 January 20

FLICKER OF EXTRAGALACTIC RADIO SOURCES AT TWO EPOCHS

J. H. SIMONETTI
Department of Physics, Virginia Polytechnic Institute and State University
AND
J. M. CORDES
Department of Astronomy, Cornell University; and the National Astronomy and Ionosphere Center
Received 1989 January 27; accepted 1989 July 17

ABSTRACT

We investigate the flicker of compact extragalactic sources on day-like time scales. Daily observations were made at 1410 MHz of 25 flat and 14 steep spectrum extragalactic radio sources during two observing sessions. The maximum time baseline for the 1410 MHz data is 58 days. We also observed these same sources at 820 MHz for 24 days overlapping the second 1410 MHz session. Ten of the flat spectrum sources were observed two years earlier at 1410 and 2380 MHz.

At 1410 MHz the flat spectrum sources show larger intensity variations than do the steep spectrum sources. At 820 MHz measurement noise dominates the source variations, thus our observations yield an upper limit to the flicker amplitude at this frequency. The flicker amplitude appears to be weakly dependent upon observing wavelength, possibly increasing with increasing wavelength. No dependence of the intensity or time scale of flicker on galactic coordinates is apparent in this data set, but the number of flat spectrum sources observed may be too small to show any such effects. We present evidence that flicker is approximately stable in its characteristics over time scales at least as large as 2 yr.

Subject headings: interstellar: matter — radio sources: variable

I. INTRODUCTION

"Flicker" of flat spectrum extragalactic radio sources at the $\sim 2\%$ level on time scales of days at 3.3 GHz was first reported by Heeschen (1984). Rickett, Coles, and Bourgois (1984) soon after put forward the hypothesis that flicker and low-frequency variability (LFV; $\sim 5\%$ variations on time scales of months to years at $\nu < 1$ GHz) are both refractive interstellar scintillations caused by electron density irregularities of size $> 10^{13}$ cm in the interstellar medium of the Galaxy. If, on the other hand, either LFV or flicker is intrinsic to the source, the source size implied by the variation time scale along with the change in flux density yields a brightness temperature in excess of the 10^{12} K limit for incoherent synchrotron sources. The current belief, based primarily on the average behavior of sets of flickering sources, is that flicker is at least partially due to refractive interstellar scintillation, and therefore instead of a presenting a problem for extragalactic source models, may be useful as a probe of the interstellar medium at large distances above the galactic plane. Similar arguments are presented for believing most LFV is scintillation (see Spangler *et al.* 1989 for details). In this paper we present additional observations of flickering sources which may be used to test the scintillation hypothesis further. Here we present the observations without interpretation in terms of a specific model.

Evidence that scintillation contributes to flicker is based on daily observations of sets of compact sources. Simonetti, Cordes, and Heeschen (1985; hereafter referred to as Paper I) attempted to test the refractive scintillation explanation of flicker, using observations over 20 days of 14 flat and 20 steep spectrum radio sources at 1410 and 2380 MHz from the Arecibo Observatory. The average structure functions of the time series for the set of flat spectrum, compact sources, showed that variations are present on time scales from 1 to greater than 20 days at both frequencies, with roughly no wavelength dependence for the modulation index (rms/mean intensity). For an extragalactic source size independent of wavelength, the predicted scintillation index (rms/mean intensity) would vary as $\sim \lambda^2$. However, as shown by Blandford, Narayan, and Romani (1986), the observed rough wavelength independence of the modulation index can be explained if the source size $\theta_{\rm sou} \propto \lambda$, and the 20 day time series were of length much less than the correlation time scale for the scintillation. Blandford, Narayan, and Romani also derived theoretical structure functions for the flicker assuming an extended scattering medium, which are in approximate agreement with the observed average structure functions. Finally, Heeschen and Rickett (1987) reanalyzed Heeschen's (1984) 23–25 day observations of compact sources and found a trend of decreasing modulation index with increasing galactic latitude of the source, discernable only because of the large number of sources examined, implying flicker is at least partially due to propagation effects within the Galaxy. There is a wide scatter of modulation index at any specific galactic latitude in their results, and this could be due to differences in source brightness distributions. In none of these observational programs, have time series of length longer than the predicted correlation time scale of the scintillations been obtained. Nor have source behaviors at vastly different epochs been examined.

Flicker studies require $\approx 1\%$ precision, nearly *daily* source measurements over at least a few weeks to yield useful information and are thus uncommon. Here we present observations at 1410 and 820 MHz of 25 flat and 14 steep spectrum sources using the National Radio Astronomy Observatory's 92 m telescope at Green Bank.[1] (Such studies may be even less common in the future now that the 92 m telescope has met its end.) The goal of the program was to test the scintillation hypothesis further, and probe the potentially responsible scattering medium by (1) reobserving at 1410 MHz a subset of the sources

[1] The National Radio Astronomy Observatory is operated by Associated Universities, Inc., under contract with the National Science Foundation.

seen to flicker in our Arecibo study, (2) observing at a lower frequency to test the proposed wavelength dependence of the modulation index over a wider frequency range, and (3) to extend the time period of the observations to attempt to find the longest time scale present in at least some of the flickering source time series. If flicker is due totally to interstellar scintillation from a medium with homogeneous statistics the expected intensity variations of an individual source should have the same statistics (viz. modulation index and fluctuation time scale) when observed at two widely space epochs, as were the Arecibo and Green Bank observations.

In § II we present the observational details and methods of obtaining the final time series of source intensity. Structure functions were computed for these time series, as discussed in § III, which are quite clearly similar to those presented in Paper I. We check for any easily discernable influence of the Galaxy's interstellar medium on the flicker process in § IV*a*, with negative, but probably inconclusive, results. In § IV*b*, we present evidence that flicker is an approximately statistically stationary process over time scales at least as great as 2 yr. Following a discussion, our conclusions appear in § VI.

II. OBSERVATIONS AND DATA REDUCTION

a) Source Selection

Roughly equal numbers of sources with unambiguously flat or steep radio spectra were chosen from the catalog of Kühr *et al.* (1979, 1981). The steep spectrum (S) sources, which have shown intensity variations consistent with zero correlation time scale noise (Paper I), are used as a control group to gauge the effective precision of the antenna temperature measurements of the flickering flat spectrum (F) sources. The only criteria used in the selection process were that: (1) a subset of the flat spectrum sources overlapped those observed for Arecibo, (2) nominal source flux densities are great enough so that radiometer noise would contribute less than $\sim 1\%$ to the uncertainty of the on-source antenna temperature measurements, and (3) as many sources as possible could be observed in a single-nighttime observing session. Additional time was available each day during the second observing session so some sources were observed only during that session. The final source list is shown in Table 1.

b) Observing Procedure

Observations were made during two separate sessions at 1410 MHz with the 1.3–1.8 GHz cooled FET receiver, utilizing linearly polarized feeds on the Sterling mount of the 92 m telescope, and during the second session at 820 MHz using the 750–1000 MHz cooled upconverter/GaAsFET receiver with dual linear feeds on the Traveling mount. In both cases the linear polarization signals were converted to circular polarization before being recorded. During the first session, we attempted observations with the 500–750 MHz receiver near 700 MHz, but a reasonably large bandpass free of interference could not be found. An observing log is presented in Table 2. At 1410 and 820 MHz, the nominal half-power beamwidths of the 92 m telescope are 10$'$.6 and 18$'$.3, while the system temperatures are ~ 25 and 80 K.

Daily drift scans were recorded for each source using the Digital Continuum Receiver (DCR; Fisher 1984) in "total power" mode. At both frequencies the receiver bandwidth was 40 MHz, integration time was 0.3 s, and the sampling time interval was 0.3 s. The DCR recorded calibrated antenna temperatures using, for this observing program, a calibration noise signal fired for 1.2 s before the start of the source scan. The noise signals were 1.87 K for both of the circularly polarized signals at 1410 MHz, and 6.53 and 5.88 K for the oppositely polarized signals at 820 MHz. All scans were taken at nighttime to avoid any detrimental effects on precision which is due to uneven solar heating of the telescope (significant at least at 3.3 GHz as noted by Heeschen 1984). When both frequencies were being observed, the Sterling and Traveling mounts were arranged so one continuous drift scan would take the source through each beam in turn, while the DCR recorded calibrated antenna temperatures in all four channels. The drift scans were of sufficient length to leave a baseline equivalent to at least 2 half-power beamwidths on either side of the 820 MHz beam response to a point source, and at least 3 half-power beamwidths on either side of the 1410 MHz beam response.

c) Data Reduction

Scans for the two polarizations and two frequencies were processed separately. We fitted a linear baseline through two prechosen portions of each scan on either side of the expected beam response (the portions were the same for each scan and each source, but different for the two frequencies), and fitted a parabola to the upper quarter of the peak beam response. The difference of the maximum of the parabola and the linear baseline at the position of the peak of the parabola was taken to be the raw antenna temperature for that scan.

After results from scans showing obvious interference effects were removed, a slight systematic difference ($\sim 2\%$) was noted between the mean antenna temperature values for the steep spectrum sources obtained at 1410 MHz during the first session, and those of the same S sources obtained during the second session. Furthermore, when we obtained the time series of antenna temperature normalized by the mean over the series for each S source, slight day-by-day systematic variations (less than $\sim 1\%$) were present throughout the S sources for both polarizations and both frequencies. Therefore, the normalized antenna temperature series were averaged over the set of S sources to produce a series, for each polarization and each frequency, which was used to calibrate out any systematic errors in the time series of any individual S or F source, and to adjust for the slight difference in system sensitivity for the two polarizations. Thus, time series of now completely calibrated antenna temperatures were produced for each source at both frequencies and polarizations. For each source a final antenna temperature time series for each frequency was produced by averaging the results for the two orthogonal polarizations.

Figure 1 shows representative time series of antenna temperature for a flat and a steep spectrum source. The observed modulation index m (rms/mean antenna temperature) for each source is presented in Table 1. In this paper m will be reserved for the *modulation index* of a time series, and the term *flicker index* will be used to refer to an observed fractional variation in intensity of a source that is corrected for measurement error contributions (i.e., caused only by flicker). The flicker index will be represented by μ to distinguish it from the modulation index.

Given the ≈ 1 K Jy^{-1} sensitivity of the 92 m telescope, and the above receiver parameters, the expected random noise variations in the measured peak response to a 0.2 Jy point source—after averaging both calibrated channels—is under 1% at 1410 MHz and a bit above 1% at 820 MHz. The pointing accuracy of 30$''$ is not a significant source of error for the above beamwidths.

TABLE 1

OBSERVED SOURCES

							820 MHz[a]			1410 MHz[a]		
SOURCE	R.A. (1950)	DECLINATION (1950)	l^{II}	b^{II}	C[c]	α[b]	m (%)	$\langle T \rangle$ (K)	S_ν (Jy)	m (%)	$\langle T \rangle$ (K)	S_ν (Jy)
0007+171......	00h07m59s8	17°07′38″	109°2	−44°4	F	−0.2	4.6	0.43	0.6	2.4	0.71	0.7
0119+115......	01 19 03.1	11 34 10	134°6	−50°4	F	0.3	6.1	0.71	1.0	1.5	0.93	0.9
0147+187......	01 47 05.5	18 42 26	141°6	−41°8	F	−0.2	5.3	0.44	0.5	2.9	0.34	0.6
0202+149......	02 02 07.4	14 59 51	147°9	−44°0	F	0.3	2.1	2.67	4.6	2.5	4.00	3.9
0235+164......	02 35 52.6	16 24 05	156°8	−39°1	F	−1.1	4.8	0.47	0.6	2.6	0.82	0.9
0250+178......	02 50 46.2	17 53 30	159°6	−35°9	F	−0.2	...	...	...	11.8	0.46	0.5
0317+188......	03 17 00.3	18 50 38	164°9	−31°5	F	−0.9	...	...	...	2.0	0.39	0.4
0430+052......	04 30 31.6	05 15 00	190°4	−27°4	F	0.0	2.4	2.32	4.6	2.3	3.61	4.6
0446+112......	04 46 21.2	11 16 19	187°4	−20°7	F	−0.5	4.2	0.68	0.6	10.3	0.64	0.8
0528+134......	05 28 06.8	13 29 43	191°4	−11°0	F	−0.5	5.5	0.77	1.6	5.5	2.13	2.1
0642+449......	06 42 53.1	44 54 29	171°1	17°9	F	0.0	...	...	...	1.0	0.54	1.0
0711+356......	07 11 05.6	35 39 53	182°2	19°7	F	−0.4	5.9	0.66	1.5	1.4	1.44	1.9
0735+178......	07 35 14.1	17 49 09	201°8	18°1	F	0.1	3.6	0.81	2.3	4.4	1.79	2.2
0839+187......	08 39 14.1	18 46 27	207°3	32°5	F	0.0	...	...	...	3.7	1.26	1.2
0923+392......	09 23 55.3	39 15 24	183°7	46°2	F	−0.1	4.5	0.92	2.7	1.1	2.99	2.8
0935+254......	00 53 59.7	25 29 34	205°5	51°0	F	−0.1	3.8	0.93	0.8	...	...	...
1055+018......	10 55 55.3	01 50 04	251°5	52°8	F	0.1	2.5	1.97	4.0	1.5	2.72	3.8
1127−145......	11 27 35.7	−14 32 55	275°3	43°6	F	0.0	2.8	3.29	6.8	1.7	4.76	6.8
1145−071......	11 45 18.7	−07 08 00	276°6	52°2	F	−0.2	5.1	0.74	0.8	2.1	0.95	0.9
2113+293......	21 13 20.6	29 21 05	76°6	−13°3	F	−0.4	...	...	...	5.1	0.76	0.9
2144+092......	21 44 42.5	09 15 51	65°8	−32°3	F	−0.1	7.6	0.50	0.9	4.1	0.74	0.9
2216−038......	22 16 16.3	−03 50 43	59°0	−46°6	F	0.4	3.4	0.87	1.2	6.1	1.66	1.0
2251+158......	22 51 29.5	15 52 54	86°1	−38°2	F	0.0	1.7	7.51	12.0	1.5	12.39	12.0
2328+107......	23 28 08.6	10 43 46	93°1	−47°1	F	0.1	3.9	0.67	1.1	4.2	1.10	1.0
2344+092......	23 44 03.8	09 14 06	97°5	−50°1	F	0.2	1.6	1.33	2.3	1.4	1.86	2.1
0030+196......	00 30 01.3	19 37 23	116°9	−42°8	S	0.6	3.1	1.51	2.6	0.7	1.95	1.9
0219+082......	02 19 22.3	08 13 05	157°8	−48°2	S	0.8	2.5	2.16	4.0	1.1	2.30	2.6
0333+128......	03 33 40.5	12 52 40	173°2	−33°3	S	0.8	2.5	1.80	3.1	0.8	2.06	2.0
0356+144......	03 56 13.6	14 27 16	176°3	−28°3	S	0.9	3.1	1.15	2.1	2.0	1.13	1.3
0411+141......	04 11 40.9	14 08 56	179°3	−25°7	S	0.7	1.3	2.02	3.2	1.2	2.29	2.2
0511+008......	05 11 31.7	00 53 13	200°4	−21°0	S	0.8	3.3	2.57	4.9	1.5	2.60	3.2
0758+143......	07 58 45.0	14 23 04	207°6	21°8	S	0.9	2.7	2.42	4.4	0.6	2.49	2.7
0818+179......	08 18 52.4	17 57 50	206°1	27°7	S	0.7	3.1	1.37	2.6	1.1	1.76	1.8
0855+143......	08 55 55.7	14 21 24	214°0	34°5	S	0.8	3.1	1.54	4.2	0.7	2.51	2.7
1014+277......	10 14 59.0	27 46 59	203°2	56°0	S	0.9	3.3	1.11	2.3	1.1	1.29	1.4
1039+029......	10 39 04.7	02 58 18	245°5	50°5	S	0.7	2.6	2.42	4.1	0.7	2.65	2.8
2128+090......	21 28 55.9	09 00 13	62°7	−29°4	S	0.8	6.2	0.77	1.3	2.0	0.97	0.9
2159+043......	21 59 29.1	04 21 41	64°2	−38°2	S	0.7	3.0	1.33	2.5	1.2	1.45	1.7
2309+184......	23 09 36.5	18 29 09	92°5	−38°2	S	1.0	1.9	1.54	3.3	1.3	1.84	1.9

[a] For each frequency, we list: m = rms/mean of the observed antenna temperature time series (the modulation index), $\langle T \rangle$ = the mean antenna temperature, and S_ν = a nominal flux density estimated from the spectrum in Kühr *et al.* 1979.

[b] Spectral index from $S_\nu \propto \nu^{-\alpha}$, estimated from the spectrum in Kühr *et al.* 1979.

[c] Spectral class: F (flat spectrum) or S (steep spectrum).

At 1410 MHz, the steep and flat spectrum sources have a similar range of mean antenna temperatures, while the modulation indexes of the steep spectrum sources are less than those of the flat spectrum sources. For this frequency we take the precision of our antenna temperature measurements to be given by the mean modulation index of the steep spectrum sources, namely 1.1% (see Table 3). At 820 MHz, the flat spectrum sources have mean antenna temperatures mostly less than 1 K, while the mean antenna temperatures of the steep spectrum sources are virtually all greater than 1 K. Furthermore, unlike in the 1410 MHz case, the modulation indexes of the entire set of sources observed at 820 MHz are approximately inversely proportional to mean antenna temperature, suggesting the results are dominated by receiver noise. Therefore, at 820 MHz we conservatively take the mean modulation index of the flat spectrum sources (4.1%) to be both the precision of our antenna temperature measurements and an upper limit to the flicker amplitude of those sources (see Table 3).

TABLE 2

OBSERVING LOG

Session	Inclusive dates[a]	Frequency (MHz)
1......	1985 Nov 01–12	1410
2......	1988 Dec 06–30	820
....	1988 Dec 12–30	1410

[a] The night of 1985 Nov. 01–02 is considered day 9 of the program (for historical reasons) on up to day 67 which is the night of 1985 Dec. 29–30.

III. STRUCTURE FUNCTION RESULTS

Structure functions were calculated for the time series (normalized by the observed mean) for each source, at each

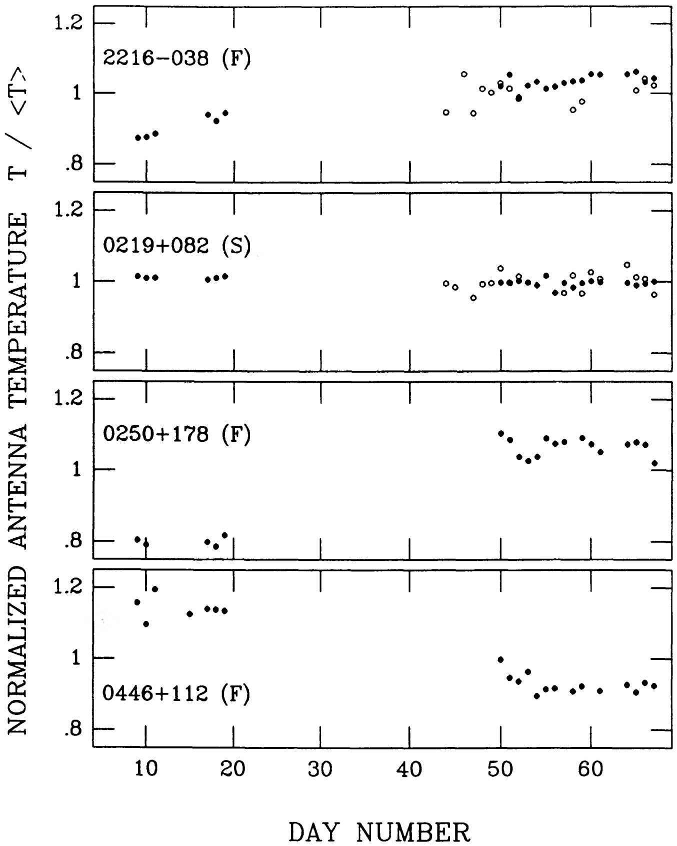

FIG. 1.—Representative time series of antenna temperature, normalized by their means, and plotted to the same scale. F and S label flat and steep spectrum sources, respectively. Filled points are data taken at 1410 MHz; open circles are data at 820 MHz. The sources 0250+178 and 0446+112 were observed to have the largest modulation indexes m at 1410 MHz.

frequency. The structure function for time series $f(t)$ and time lag τ is calculated as (see Paper I)

$$D(\tau) = \langle [f(t+\tau) - f(t)]^2 \rangle_{\text{average over } t} . \tag{1}$$

If the shortest and longest time scales in $f(t)$ are τ_S and τ_L, and the observed time series is much longer than τ_L, then

$$D(\tau) \propto \begin{cases} \text{constant} , & \text{if } \tau > \tau_L , \\ \tau^2 , & \text{if } \tau < \tau_S , \\ \tau^x , x \le 2 , & \text{if } \tau_S < \tau < \tau_L . \end{cases} \tag{2}$$

Where $D(\tau)$ is constant, τ is greater than τ_L, the correlation or *saturation* time scale in the series; $D(\tau) \propto \tau^2$ indicates $\tau <$ the smallest time scale present; and the occurrence of a range of τ where $D(\tau) \propto \tau^x$ for $0 < x < 2$ implies there are a range of time scales present in the time series. Random, uncorrelated measurement noise adds a constant value of $2\,\sigma_n^2$ to the structure function at all lags, where σ_n^2 is the variance of the noise.

The grand-average structure functions over all F and S sources at the two frequencies are shown in Figure 2. The S source results are consistent with a measurement noise process (zero correlation time scale), and are consistent with the noise levels from Table 3 of 1.1% and 3.0% at 1410 and 820 MHz, respectively. At 820 MHz, the F source results are also consistent with time series dominated by uncorrelated measurement noise, at a level of 4.1%, as we suggested in the last section. On the other hand, at 1410 MHz, the F source results are similar to the results of our previous program (Paper I), in that they indicate the presence of flicker on a range of time scales, where now there is some indication of reaching the largest time scale, on average, near 30 days.

At 820 MHz we have obtained an upper limit to the flicker index at 4.1% from our observations of the flat spectrum sources. The mean modulation indexes listed in Table 3 may be used to estimate the average flicker index to assign the flat spectrum sources at 1410 MHz. Estimated as $\mu = (\langle m \rangle_F^2 - \langle m \rangle_S^2)^{1/2}$, the flicker index for the flat spectrum sources

TABLE 3

OBSERVED MODULATION INDEXES

FREQUENCY (MHz)	STEEP SPECTRUM		FLAT SPECTRUM	
	$\langle m(\%)\rangle$[a]	σ_m	$\langle m(\%)\rangle$	σ_m
820..........	3.0	1.1	4.1	1.6
1410..........	1.1	0.5	3.5	2.8

[a] Referred to as $\langle m \rangle_s$ throughout this paper and adopted, at 1410 MHz, as the measurement uncertainty contribution (along with flicker) to the variations in the flat spectrum (F) sources. Variation indexes corrected for this measurement uncertainty are labeled by μ.

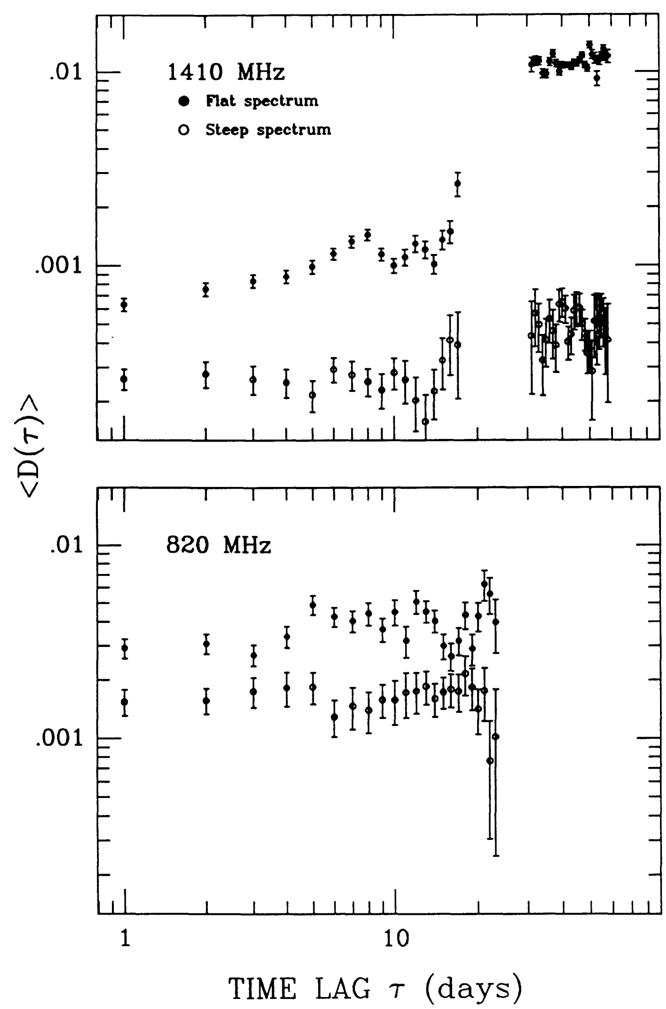

FIG. 2.—Grand-average structure functions. The value at any lag is the mean over the designated set of individual source structure functions; error bars are $\pm 1\,\sigma$ uncertainty in the mean.

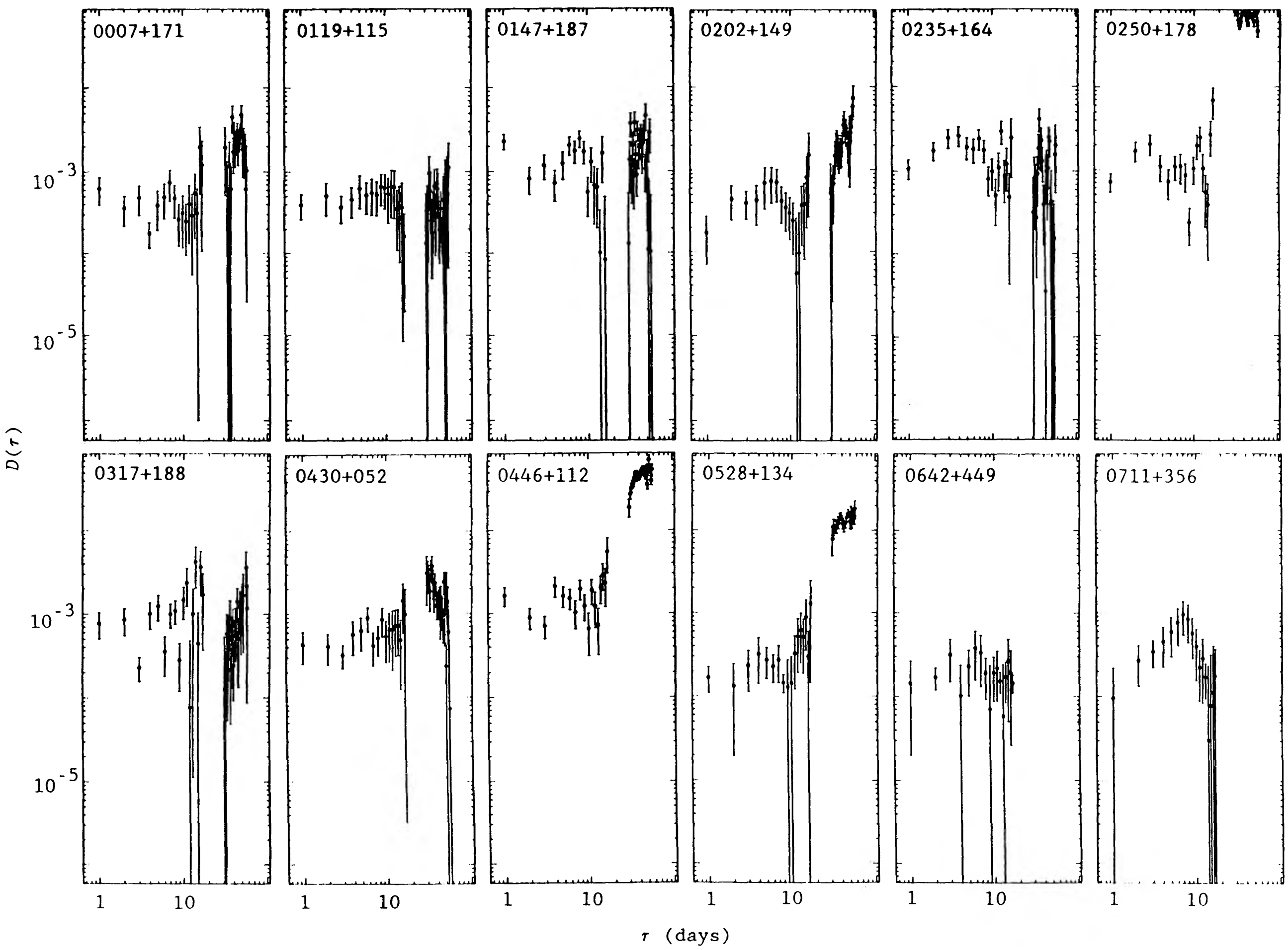

FIG. 3.—The flat spectrum source structure functions at 1410 MHz

at 1410 MHz is 3.3% for these observations. Since the 1410 MHz time series are considerably longer than those at 820 MHz, and may approach or exceed the saturation time scale for some sources, to obtain a wavelength dependence for μ where both time series are of comparable length it is more appropriate to compare the 820 MHz upper limit from these observations with the 1410 MHz result from Arecibo. Of course, in this case we are comparing results of observations of two different sets of flat spectrum sources, but 10 sources are in common to the set of Arecibo sources (14 in all) and the Green Bank sources (25 in all). If the two different sets are reasonably representative of flat spectrum sources in general, such a comparison may be justified. From Paper I, at 1410 MHz $\langle m \rangle_F = 2.26\%$, $\langle m \rangle_S = 1.02\%$, yielding $\mu = 2.0\%$. Thus, the 1410 MHz Arecibo results and the 820 MHz Green Bank upper limit imply an upper limit to the ratio μ_{820}/μ_{1410} of 2.1, for admittedly different sets of flat spectrum sources. Alternatively, we conclude the ficker index can increase no faster, with increasing wavelength, than $\mu \propto \lambda^{1.4}$. Blandford, Narayan, and Romani (1986) conclude $\mu \propto \lambda^{1/2}$ for time series shorter than the saturation time scale, or $\mu_{820}/\mu_{1410} = 1.3$, which is not ruled out by our upper limit.

In the remainder of the paper, we will only treat the 1410 MHz data. Structure functions for each of the F sources at 1410 MHz are shown in Figure 3. Table 4 presents values of μ and τ_{sat} estimated for a subset of the flat spectrum sources observed at 1410 MHz where any discernable time structure could be found in the structure function.

IV. THE CHARACTERISTICS OF FLICKER

a) *Flicker versus Galactic Coordinates*

If propagation effects within the Galaxy contribute to flicker, the statistical properties of the flicker of a set of similar sources should show a dependence upon galactic latitude and possibly galactic longitude as well.

Figure 4 displays a plot of the square of the flicker index ($\mu^2 = m^2 - \langle m \rangle_s^2$) at 1410 MHz, for the entire set of observed flat spectrum sources. The scatter in this diagram either hides any dependence of flicker on the galactic line of sight, or perhaps demonstrates the dominant role intrinsic effects play in flicker. However, it is more likely the number of observed sources is too small to show any trend which is due to a galactic influence, if there is one, Heeschen and Rickett (1987), in a similar analysis of flicker observations, obtained a weak latitude dependence from a set of ~ 180 independent values of μ^2 versus galactic latitude, ~ 10 times as many data points as we present here. We can apparently do no better finding any dependence of flicker index on galactic longitude (Fig. 5), or dependence of saturation time scale τ_{sat} (from Table 4) on latitude or longitude (Figs. 6 and 7). Two sources (0250+178 and 0446+112) have considerably larger flicker indexes than the

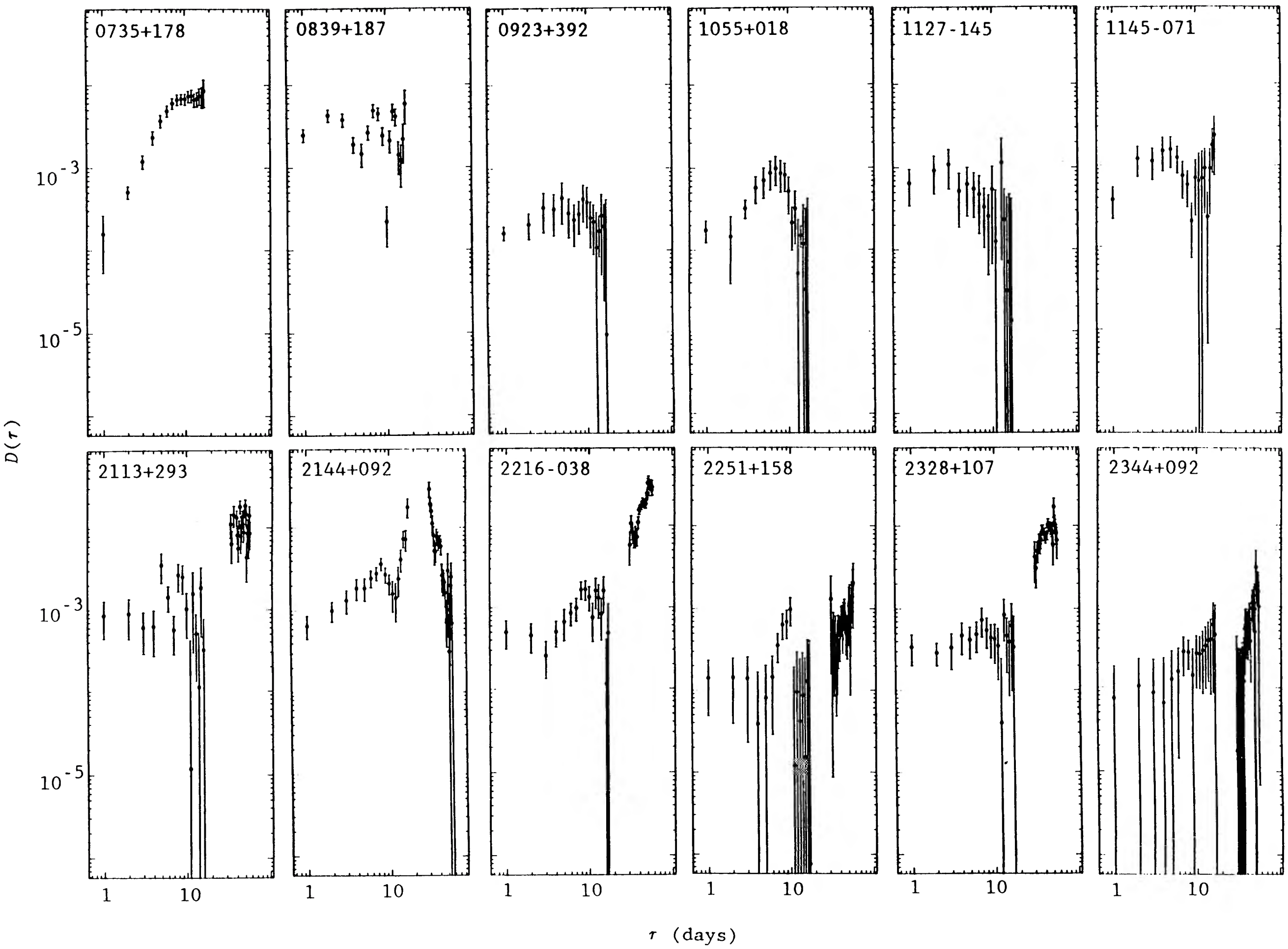

FIG. 3—*Continued*

rest of the F sources, and although they are located within $\sim 30°$ of each other, there is no cause to consider their behavior indicative of any Galactic influence (they are 21° and 36° below the galactic plane, $\sim 30°$ apart, and in the direction of the anticenter). It is also quite possible that our time series are not long enough to accurately estimate μ and τ_{sat}, which may contribute to the scatter in the diagrams. This is most likely to be true for the τ_{sat} results. However, we argue below that μ is probably known to within a factor of 2 from our observations.

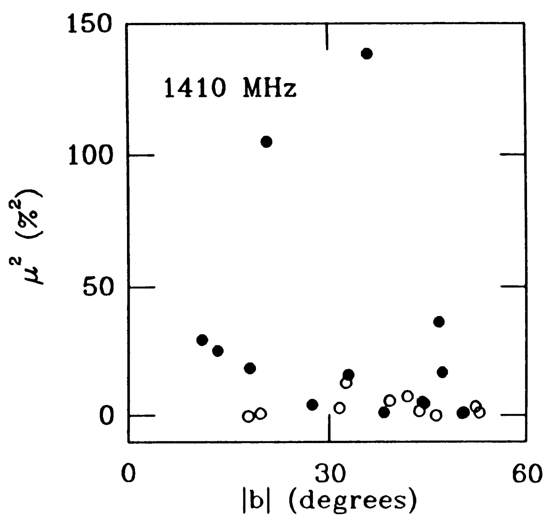

FIG. 4.—Squared flicker index ($\mu^2 = m^2 - \langle m \rangle_S^2$) vs. galactic latitude for flat spectrum sources at 1410 MHz. Filled points are for sources with characteristic time scales listed in Table 4.

b) Flicker Behavior Over a Two-Year Period

It is important to test whether flicker is stationary, because scintillation would be expected to show stationary statistics in at least the simplest of models (viz. scattering medium with homogeneous statistics). Nonstationary flicker may exclude such models. On the other hand, while some types of intrinsic variability seem to display nonstationary behavior (e.g., bursts), stationary flicker behavior would not rule out a contribution to flicker by some stationary intrinsic process.

There are 10 flat spectrum sources in common to this observing program (carried out during 1985) and our previous program at Arecibo during 1983 (Paper I). In Figure 8 we present the average structure function for the 10 sources in common as observed during the two epochs. The error bars represent $\pm 1\ \sigma$ uncertainty in the mean value at a specific lag. It is important to realize, when comparing these two structure functions, that structure function values at successive lags are correlated, which results in apparent trends, dips, or rises, which may seem real since they extend over a number of lags. False trends would disappear from average structure functions

TABLE 4

OBSERVED FLICKER INDEX AND TIME SCALE AT 1410 MHz

Source[a]	b^{II}	m[b] (%)	μ[c] (%)	τ_{sat}[d] (days)
0007+171..........	−44°4	2.4	2.1	>60
0202+149..........	−44.0	2.5	2.2	>60
0250+178..........	−35.9	11.8	11.7	30
0430+052..........	−27.4	2.3	2.0	30
0446+112..........	−20.7	10.3	10.2	45
0528+134..........	−11.0	5.5	5.4	>60
0735+178..........	18.1	4.4	4.3	8
2113+293..........	−13.3	5.1	5.0	30
2144+092..........	−32.3	4.1	3.9	30
2216−038..........	−46.6	6.1	6.0	>60
2251+158..........	−38.2	1.5	1.0	>60
2328+107..........	−47.1	4.2	4.1	55
2344+092..........	−50.1	1.4	0.9	>60

[a] Only for those flat spectrum sources where the observed structure function showed any rise with increasing time lag and the maximum time lag was greater than 20 days. However, one source with maximum time lag less than 20 days was included (0735+128), since its structure function was considerably above the noise level determined by the steep spectrum sources.

[b] The observed modulation index of the time series. see Table 1.

[c] The flicker index, calculated as $\mu = (m^2 - \langle m \rangle_s^2)^{1/2}$, to correct for antenna temperature measurement uncertainty estimated as $\langle m \rangle_s = 1.1\%$ from the steep spectrum modulation indexes.

[d] The saturation time scale for the source, taken as the time lag at which its structure function begins to level off.

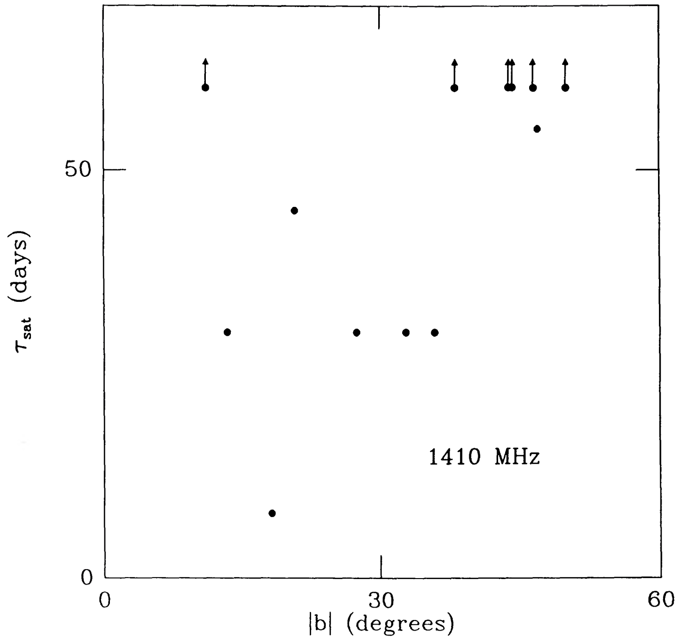

FIG. 6.—Saturation time scales for sources in Table 4 plotted vs. galactic latitude.

taken over larger and larger sets of sources. For a small set of sources, it is dangerous to place too much confidence in the appearance of features in an average structure function. This comment also applies to any interpretation of features in the grand-average structure functions plotted in Figure 2. In short, the most conservative statement is that the two structure functions in Figure 8 are consistent, given the displayed error bars. Concerning detailed behaviors, the larger $D(\tau)$ value at $\tau = 1$ day in the Green Bank result is due almost entirely to the 1 day lag result for 0146+187 dominating the average. At lags near 10 days, the marked difference in the average structure functions can be attributed to the different behaviors of 0235+164 and 2144+092 on such lags at the two epochs. On the whole the sources behave similarly at the two epochs. Figure 9 shows the individual source structure functions from the Arecibo data (compare with the corresponding plots in Fig. 3).

In Table 5 we list these 10 sources along with measures of their flicker variability derived in three different ways. One of

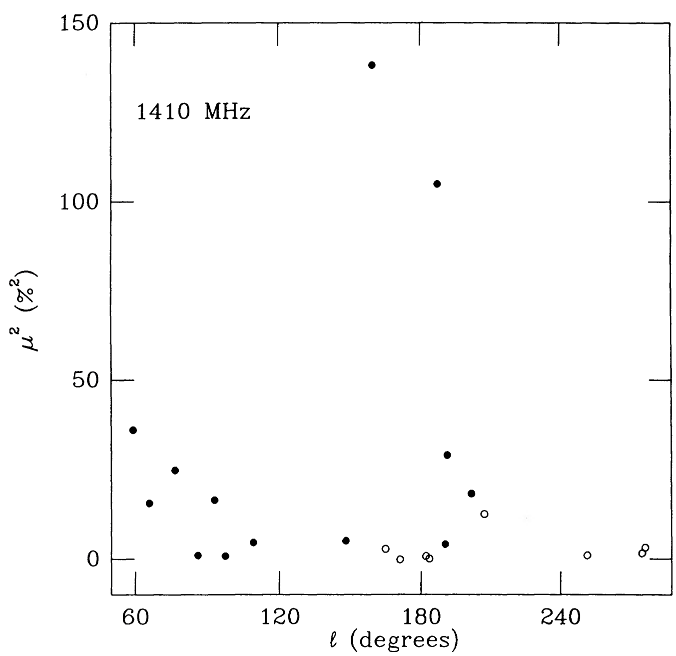

FIG. 5.—Squared flicker index ($\mu^2 = m^2 - \langle m \rangle_S^2$) vs. galactic longitude for flat spectrum sources at 1410 MHz. Filled data points are for sources listed in Table 4.

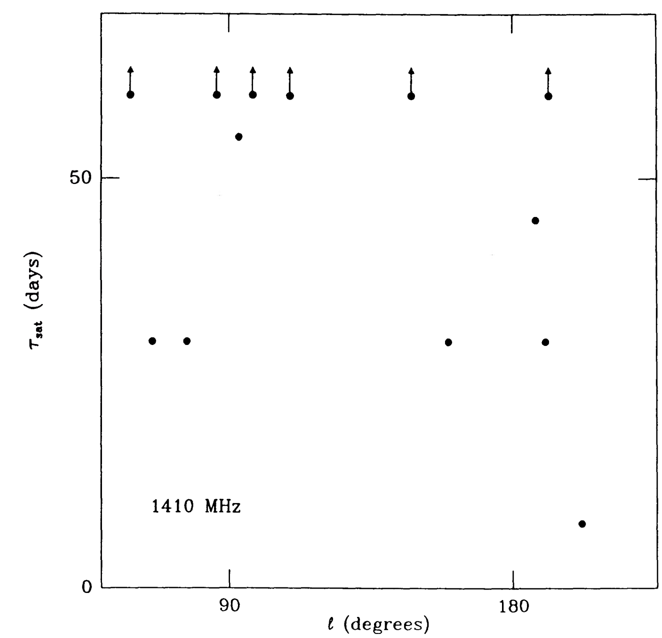

FIG. 7.—Saturation time scales from Table 4 plotted vs. galactic longitude.

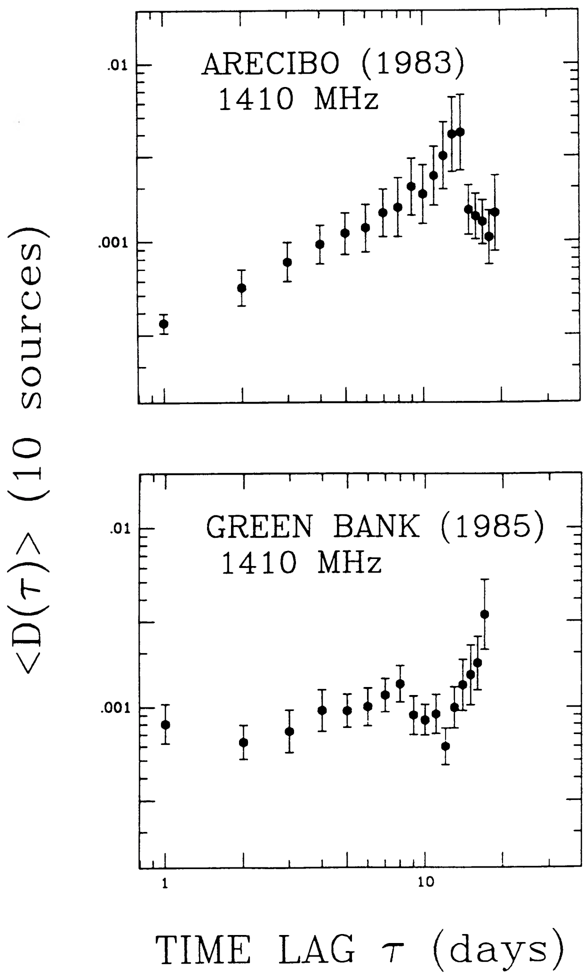

FIG. 8.—Average structure functions for the 10 flat spectrum sources in common to the Arecibo (during 1983) and Green Bank (during 1985) observing programs. The sources are listed in Table 5.

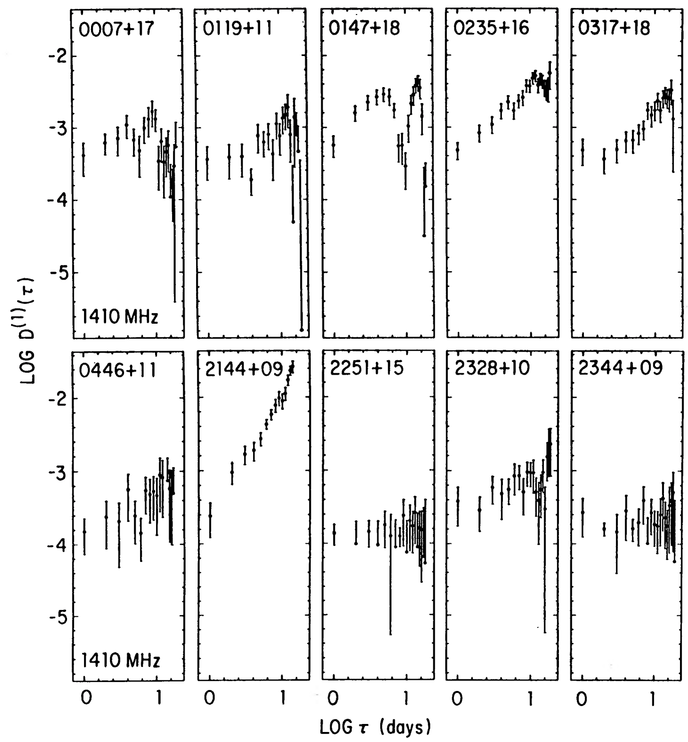

FIG. 9.—Individual source structure functions for the 10 sources listed in Table 5 as observed in the Arecibo program. Compare these with the corresponding structure functions in the Green Bank program shown in Fig. 3.

these measures is based on the 2–3 day behavior of the structure function which should be somewhat insensitive to longer time scale variability and fairly well determined given the lengths of our series. In nearly all cases the behaviors of the sources are similar at both epochs, independent of the measure of variability one prefers. Figure 10 displays the ratio of the various measures of variability at the two epochs for each of

TABLE 5

FLICKERING SOURCES AT TWO EPOCHS (1410 MHz)[a]

	1983 (ARECIBO)			1985 (GREEN BANK)		
SOURCE	μ_T[b] (%)	$\mu_{15\ \mathrm{days}}$[c] (%)	μ (from D[2.5 days])[d] (%)	μ_T[b] (%)	$\mu_{15\ \mathrm{days}}$[c] (%)	μ (from D[2.5 days])[d] (%)
0007+171......	1.5	1.6	1.5	2.1	0.7	0.7
0119+115......	1.5	1.7	1.0	1.0	1.2	1.0
0147+187......	2.7	2.2	3.0	2.7	2.1	2.0
0235+164......	3.4	4.0	2.0	2.4	2.7	3.0
0317+188......	2.2	1.4	1.0	1.7	2.0	1.3
0446+112......	1.0	1.0	0.5	10.2	2.6	1.7
2144+092......	4.8	5.0	2.3	3.9	3.1	2.0
2251+158......	<1.0	<1.0	<1.0	1.0	<1.1	<1.1
2328+107......	1.5	1.6	1.0	4.1	1.0	0.5
2344+092......	<1.0	0.5	<1.0	0.9	<1.1	<1.1

[a] These 10 sources were observed in both the Arecibo program (Simonetti, Cordes, and Heeschen 1985) and the Green Bank program.

[b] $\mu_T = (m^2 - \langle m \rangle_s^2)^{1/2}$, where m is the modulation index for the *entire* observed time series, and $\langle m \rangle_s$ is 1.0% and 1.1% for the Arecibo and Green Bank programs, respectively.

[c] Same as for μ_T but m is computed from the first 15 observing days in the Arecibo program, or the last 15 days of the Green Bank program.

[d] Same as for μ_T but $m^2 = \frac{1}{2}D(2.5\ \mathrm{days})$, where the D(2.5 days) is the average of the stucture function values at lag 2 and 3 days for that source.

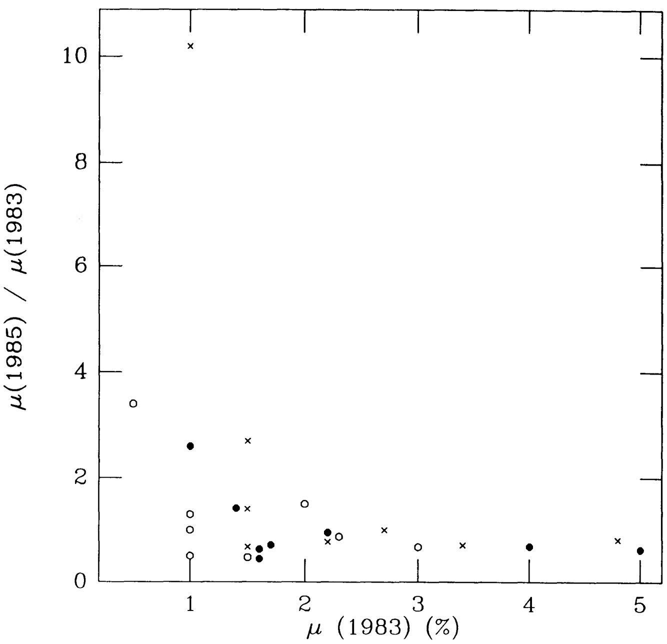

FIG. 10.—A comparison of flicker indexes from the 1983 (Arecibo) program and 1985 (Green Bank) program, as listed in Table 5. The two sources (2251 + 158 and 2344 + 092) where only upper limits were determined at one epoch were ignored, but their behaviors at both epochs are about the same, which is consistent with the results for the other sources. Crosses are points using $\mu = \mu_T$, filled circles are for $\mu = \mu_{15 \text{ days}}$, and open circles are for μ determined from D(2.5 days). One source (0446 + 112) accounts for the largest value of $\mu(1985)/\mu(1983)$ determined by the three methods. Ignoring this source (see text) leaves the other values of $\mu(1985)/\mu(1983)$ all clustered near unity, to within a factor of 2, essentially. Apparently the process producing the intensity variations is approximately the same at the two epochs.

the sources. Ignoring one source (0446 + 112), we see the calculated flicker indexes for each source are the same at both epochs to within essentially a factor of 2. The source 0446 + 112 may have quite different behaviors at both epochs, but it is hard to be completely confident in this conclusion, since the observations of this source at Arecibo in 1983 were made with an incorrect source declination (apparently off by $\sim 26''$) which severely affected the 2380 MHz observations, and may have also corrupted the 1410 MHz results. Instead, it seems prudent to ignore this source in drawing any conclusions. Thus, although the remaining source flicker indexes range over a factor of 5, the ratio $\mu(1985)/\mu(1983)$ is within a factor of 2 of unity. Ignoring 0446 + 112, and the two sources for which only upper limits to the flicker index were determined (2251 + 158 and 2344 + 092), the remaining 7 sources have a mean $\mu(1985)/\mu(1983)$ for 15 day series of 0.78 with sample standard deviation 0.33.

This mean and standard deviation are consistent with what we know about the flicker process and the conclusion that the source flicker indexes changed by less than a factor of 2 from 1983 to 1985. To confirm this we simulated random time series of length 15 days, and computed ratios of flicker indexes. A structure function approximately linear in lag is observed, on average, for flickering sources (Paper I, and Figs. 2 and 8 of this paper), while Figure 2 suggests the correlation time scale for our sources observed at 1410 MHz is near 30 days. Therefore, we generated time series of length 15 days, whose ensemble structure function would be proportional to lag at lags less than 30 days and constant at lags greater than 30 days. The flicker index for an infinitely long series $\mu(\infty)$ was a free parameter, allowing the generation of different sets of series, each set containing realizations of a process having a different flicker amplitude.

Each series in a set was generated in the following manner: (1) a random number generator produced a series of 44 uncorrelated numbers from a Gaussian distribution of zero-mean and unity variance, (2) this series was smoothed (averaged) within a running window of width 30 samples, yielding 15 final samples, (one 15 sample realization of a random process with a triangular autocorrelation function or linear structure function at lags lass than 30), (3) each sample was multiplied by $\mu(\infty)(30)^{1/2}$, and (4) the value 1 was added to each sample.

Choosing $\mu_1(\infty) = 0.046$ (for set number 1), 200 simulated series had flicker indexes μ_1 with a sample mean and standard deviation of 0.019 and 0.0085, respectively. This value of $\mu(\infty)$ corresponds to an ensemble structure function consistent with the observed average structure functions in Figure 8. A second set with $\mu_2(\infty) = 0.092$ (twice that of set 1) and 200 series, had the corresponding mean and deviation values for μ_2 of 0.037 and 0.017. It follows that ratios μ_1/μ_2 for randomly chosen pairs from the two sets would be expected to have a mean of 0.51 and standard deviation 0.33. This result is consistent with the observed $\mu(1985)/\mu(1983)$ mean and standard deviation of 0.78 and 0.33, if the 1983 series have a flicker amplitude larger on average than those of 1985, but not by more than a factor of 2. Choosing $\mu_1(\infty) = 0.075$ resulted in 200 flicker indexes μ_1 with a mean and standard deviation of 0.030 and 0.012—a sample mean equivalent to the largest such value for the sources as observed in 1983. For $\mu_2(\infty) = 2\mu_1(\infty) = 0.15$, the mean and standard deviation of μ_2 was 0.060 and 0.027. These values imply ratios of μ_1/μ_2 for random pairs would have a mean and standard deviation of 0.50 and 0.30. Again this is consistent, now for larger μ, with the observed results.

In summary, since the observed flicker index of each source (ignoring 0446 + 112) from 1983 to 1985 is the same to within a factor of 2, we conclude the flicker process was approximately the same for these sources at the two epochs.

V. DISCUSSION

Only a complete picture of flicker will fully clarify the possible intrinsic and extrinsic contributions to the observed intensity variations. We currently have evidence for the following phenomological properties of the flicker of compact extragalactic radio sources: (1) intensity variations take place on time scales ranging from at least as small as 1 day up to at least 20 days at GHz frequencies (Paper I; this paper; Heeschen 1984). At 1410 MHz fluctuations up to at least 60 days are present (this paper). Flicker variations have been detected at 2.7 GHz with time scales ranging from 4 hours to 3 days (Heeschen *et al.* 1987), and with structure functions matching up with longer time scale observations such as reported here (Heeschen *et al.* 1987). (2) The modulation index of flicker variations for time series of length ~ 20 days or more are $\sim 2\%$–3% with a slow increase in amplitude with increasing wavelength (Paper I; this paper; Heeschen 1984). (3) Flicker is apparently a broad-band phenomenon with correlated variations seen at 1410 and 2380 MHz (Paper I). (4) It appears flicker is approximately stationary over a 2 yr time period (this paper). From the work of Heeschen and Rickett (1987), we know (5) the flicker amplitude exhibits a weak dependence on galactic latitude.

While many of these properties are consistent with models explaining flicker as dominated, at the least, by refractive interstellar scintillation, contributions to the observed variations by intrinsic effects cannot be ruled out. Intensity variations on day-like time scales and shorter have been reported that are clearly not consistent with the above properties of flicker. Heeschen *et al.* (1987), along with the above mentioned hour-to-day flicker-like variations, found about one-half of their set of circumpolar compact sources exhibited a larger amplitude variation ($\sim 5\%$) on a time scales of 1–2 days. Although these sources are within a region of sky containing H I shell structures and a radio continuum loop, it is not established that the observed variations are caused by propagation effects. Dreher, Roberts, and Lehár (1986) reported a 1.8% change in the flux density of OJ287 on a seven hour time scale at 5 GHz, and de Bruyn (1988) observed a 7% drop in its flux density in just over 1 hour at 4.9 GHz. Again these variations are not consistent with an extrapolation of flicker variations to short time scales. These forms of variability may be either dominated by intrinsic effects, or indicate unusual refractive effects are taking place in some cases.

VI. CONCLUSIONS

We have made further daily observations of flickering compact extragalactic radio sources to expand the data set available for the construction and testing of the various possible models. We have not presented the observations in relation to any specific model (e.g., flicker is scintillation). Instead, in this paper the phenomenological characteristics of flicker are discussed. We would like to emphasize the following points:

1. The flicker index μ of the intensity variations for time series of length shorter than the saturation time scale of the process appears to increase slowly with increasing wavelength. Data at 820 (an upper limit to the flicker index) and 1410 MHz from the Green Bank and Arecibo data sets, respectively, imply $\mu \propto \lambda^x$, where $x < 1.4$. This result is consistent with the results at 1410 and 2380 MHz as presented in our earlier program (Paper I).

2. No dependence of the flicker index μ, or characteristic time scale $\tau_{\rm sat}$, was apparent in the 1410 MHz. This may only reflect the scatter inherent in the limited number of sources we observed and limited time series we obtained and details such as intrinsic source size and brightness distribution. On the other hand, intrinsic contributions to flicker may be present, and could always contribute to scatter in such results. These results do underline how much work must be expended in future such programs in order to potentially reduce such uncertainties.

3. From a comparison of the 1410 MHz flicker indexes of a set of 9 sources as observed from Arecibo in 1983 and from Green Bank in 1985, we found the flicker index of any particular source was the same, to within about a factor of 2, for the two epochs (ignoring a tenth source where incorrect observing coordinates were used in 1983). This suggests the flicker process is approximately the same at the two epochs.

A complete picture of flicker demands observational programs of longer duration, and more study of flicker on time scales shorter than 1 day. It would also be quite useful to obtain VLBI structures of flickering sources for use in constraining models.

It is a pleasure to thank J. J. Condon, B. K. Dennison, D. S. Heeschen, and D. R. Stinebring for helpful discussions. We also thank the staff of NRAO at Green Bank, in particular J. R. Fisher, and H. E. Payne, for help during the observing program.

REFERENCES

Blandford, R., Narayan, R., and Romani, R. W. 1986, *Ap. J. (Letters)*, **301**, L53.
de Bruyn, A. G. 1988 in *IAU Symposium 129, The impact of VLBI on Astrophysics and Geophysics*, ed. M. J. Reid and J. M. Moran (Dordrecht: Kluwer), p. 97.
Dreher, J. W., Roberts, D. H., and Lehár, J. 1986, *Nature*, **320**, 239.
Fisher, J. R. 1984, NRAO Electronics Division Internal Report, No. 243.
Heeschen, D. S. 1984, *A.J.*, **89**, 1111.
Heeschen, D. S., Krichbaum, Th., Schalinski, C. J., and Witzel, A. 1987, *A.J.*, **94**, 1493.
Heeschen, D. S., and Rickett, B. J. 1987, *A.J.*, **93**, 589.
Kühr, H., Nauber, U., Pauliny-Toth, I. I. K., and Witzel, A. 1979, Max-Planck-Institut für Radioastronomie preprint, No. 55.
Kühr, H., Witzel, A., Pauliny-Toth, I. I. K., and Nauber, U. 1981, *Astr. Ap. Suppl.*, **45**, 367.
Rickett, B. J., Coles, W. A., and Bourgois, G. 1984, *Astr. Ap.*, **134**, 390.
Simonetti, J. H., Cordes, J. M., and Heeschen, D. S. 1985, *Ap. J.*, **296**, 46 (Paper I).
Spangler, S., Fanti, R., Gregorini, L., and Padrielli, L. 1989, *Astr. Ap.*, **209**, 315.

JAMES M. CORDES: Space Sciences Building, Cornell University, Ithaca, NY 14853

JOHN H. SIMONETTI: Physics Department, Virginia Polytechnic Institute and State University, Blacksburg, VA 24061